List of Supplementary Figures

Supplementary Figures Legends

Supplementary Figure 1: Intracellular metabolite concentration profiles during the acidogenic-solventogenic transition

The concentration (mM) or relative concentration profiles of the metabolites used for the generation of Figure 1B are shown. The data correspond to the fermentation time points shown in Figure 1A, starting at 4h. The error bars show ± standard error (n = 2 replicate measurements).

Supplementary Figure 2: Progressive metabolome remodeling during the acidogenic-solventogenic transition: independent biological replicates.

(A) Fermentation profile and growth curve obtained in three independent, pH=4.7 controlled batch cultures. Fermentation *A* was used as the representative dataset in Figure 1.

(B) Metabolome dynamics during the acidogenic-solventogenic transition in three independent experiments. Unsupervised hierarchical cluttering analysis of 114 intracellular metabolite levels. Rows represent specific intracellular metabolites. Columns correspond to the fermentation time points shown in (A). Relative metabolite concentrations across time points are normalized to have a mean equal to zero and standard deviation equal to 1. Metabolites whose levels are higher than the mean across time points are shown in shades of yellow and those with lower levels than the mean in shades of blue. In each fermentation, the data represents the average of two replicate LC-MS measurements. Metabolite extractions from Fermentations *A* and *C* were performed using the rapid filtration method; metabolite extractions from Fermentation *B* were performed using the direct quenching method (see methods section). Hexose-phosphate represents the combined pools of glucose-6-phosphate and fructose-6-phosphate. Phosphoglycerate represents the combined pools of glycerate-2-phosphate and glycerate-3-phosphate.

Supplementary Figure 3: Extracellular metabolites during the solventogenic transition: Independent biological replicates

(A) Unsupervised hierarchical cluttering analysis of extracellular metabolite data in three independent, pH=4.7 controlled batch cultures. Rows represent specific metabolites. Columns correspond to the fermentation time points shown in Supplementary Figure 2A. Extracellular metabolite levels across time points are normalized to have a mean equal to zero and standard deviation equal to 1. Concentrations that are higher than the mean across time points are shown in shades of yellow and those lower than the mean in shades of blue. Grey indicates missing data. For each fermentation, the data represents the average of two replicate measurements. Hexose-phosphate represents the combined pools of glucose-6-phosphate and fructose-6-phosphate.

Supplementary Figure 4: Comparison of intracellular metabolome profiles between fermentations at pH=4.7 vs. pH=6.0

(A) Fermentation profiles and growth curves obtained in pH=4.7 and pH=6.0 controlled batch cultures. At pH=6.0 there is a very small period where butanol is produced as the cells exit exponential growth. There is however, no overt solventogenic phase and no acid reuptake.

(B) Comparison between the metabolome dynamics of pH=4.7 and pH=6.0 controlled batch cultures. Columns correspond to the fermentation time points shown in (A), starting at 4 h. The metabolome pattern during acidogenesis is similar in both cultures but then diverges markedly as the low pH culture enters solventogenesis. Relative metabolite concentrations across time points are normalized to have a mean equal to zero and standard deviation equal to 1. Metabolites whose levels are higher than the mean across time points are shown in shades of yellow and those with lower levels than the mean in shades of blue. In each fermentation, the data represents the average of two replicate measurements. Hexose-phosphate represents the combined pools of glucose-6-phosphate and fructose-6-phosphate. Phosphoglycerate represents the combined pools of glycerate-2-phosphate and glycerate-3-phosphate.

Supplementary Figure 5: Comparison of extracellular metabolite profiles between fermentations at pH=4.7 and pH=6.0

Fermentation profile and extracellular metabolome composition in fermentations carried out at pH=6.0 (A) and pH=4.7 (B). The extracellular composition graphs show the molar abundance of 50 different metabolites, most of them combined as groups of metabolites. For each fermentation, the data represents the average of two replicate measurements. The data in (B) corresponds to Fermentation *B* in Supplementary Figure 2.

Supplementary Figure 6: Metabolic impact of exogenous acid addition

(A) Metabolome dynamics after the addition of butyrate (30 mM) and acetate (30 mM) to exponentially growing cells (OD_{600}=0.6, pH=6.0). The pH was dropped to 4.7 simultaneously with the addition of butyrate and acetate. This treatment did not trigger solvent production (as determined by 1D proton NMR measurements) and, with the exception of a few metabolites, did not reproduce the metabolic changes observed during acidogenesis or early solventogenesis. Relative metabolite concentrations across time points are normalized to the mean and standard deviation of the pH=4.7 fermentation time course. The data for the fermentation at pH=4.7 corresponds to the one shown in Figure 1. The data for the addition of acetate and butyrate represents the average of two measurements from two parallel cultures.

(B) Selected concentration profiles after butyrate and acetate addition. The data for the addition of acetate and butyrate represents the average from two parallel cultures. The error bars show ± standard error.

Supplementary Figure 7: Metabolome changes in butanol treated cells

(A) At T=0, exponentially growing cells (OD_{600}=0.6, pH controlled at 6.0) were treated by addition of butanol (70mM). The graph shows the ratio of the total concentration of all secreted metabolites (excluding acetate and butyrate) in butanol-treated cells over control cells.

(B) Intracellular metabolite concentration profiles after butanol addition. The data represents $\log_2$ fold-change against T=0 and is an average of 2 independent measurements from a single culture. An independent experiment (not shown) was performed with comparable results.

(C) Selected metabolites after butanol addition and comparison with their respective concentration profiles during the acidogenic-solventogenic transition. The error bars show ± standard error.

Supplementary Figure 8: Interchange between the intracellular acetyl-CoA pool and the extracellular acetate pool during acidogenesis

(A) Dynamic incorporation of extracellular U-^{13}C-acetate into acetyl-CoA, butyryl-CoA and acetylphosphate. The *x* axis represents minutes after the addition of U-^{13}C-acetate and the *y* axis represents the ^{13}C-labeled fraction (sum of all different labeled forms) of the indicated metabolite. The data represents the average from two parallel cultures.

(B) Using a filter culture methodology (2, 42) acidogenic cells were switched (at T=0) to fresh media containing 100% U-^{13}C-labeled glucose but no extracellular acetate or butyrate. Rapid and complete labeling of acetyl-CoA and butyryl-CoA is observed. The data represents the average from two parallel cultures.

(C) Long term incorporation of ^{13}C-labeled glucose. At time=0, universally ^{13}C-labeled glucose was added into mid-exponential cultures in a matching amount to the non-labeled glucose remaining in the media to reach a 1:1 ratio between ^{13}C-labeled and non-labeled glucose. The line graphs represent the ^{13}C-labeled fraction (sum of all different labeled forms) of the indicated metabolite as a function of time. The labeling dynamics of these metabolites is biphasic, reaching a very rapid initial equilibrium (within less than 5 minutes) at a low ^{13}C-labeled fraction, which then increases slowly as the extracellular fraction of ^{13}C-labeled acetate and butyrate increases over time. The data shown is one dataset representative of two independent acidogenic cultures. The complete dataset is included in Supplementary Table 3.

Supplementary Figure 9: Assimilation of extracellular ^{13}C-fumarate during the acidogenic-solventogenic transition

U-^{13}C-fumarate was added to cells undergoing the acidogenic-solventogenic transition during the time at which extracellular fumarate is re-assimilated. The *y* axis represents the ^{13}C-labeled fraction (sum of all different labeled forms) of the indicated metabolite. The error bars show ± standard error (n = 2 independent experiments). We have previously established that glutamate biosynthesis in *C. acetobutylicum* occurs exclusively via the oxidative TCA cycle and aspartate biosynthesis exclusively via oxaloacetate (2). Therefore, the incorporation of ^{13}C-labeled fumarate into malate, glutamate, and aspartate implies its metabolism through the TCA cycle.

Supplementary Figure 10: Reactions of the ordinary differential equation model.

F1 and F14 represent the sums of multiple amino acid producing fluxes. Shaded italic items (i.e. other outflux from glycolysis, Asp, or Glu) represent carbon utilization in processes not included in the ODE equations such as the pentose phosphate pathway, nucleotide biosynthesis, lipid biosynthesis, etc.

Supplementary Figure 11: The distribution of the one thousand sets of fluxes that reproduce the experimental labeling dynamics.

The distribution of the one thousand sets of fluxes that quantitatively describe the laboratory data in two independent acidogenic and two independent solventogenic cultures. A narrower distribution indicates that the corresponding model parameter is identified (from experimental labeling dynamics, Figure 4 and Supplementary Table 3) with lower uncertainty, while a broader distribution represents the opposite. In most of the cases, broad distributions are associated with exchange fluxes, which is reasonable because the experiments were not specifically designed to constrain them. The units in the *x*-axis are in Log_{10} (micro-mol.min-1.gCDW-1).

Supplementary Figure 1 (1)

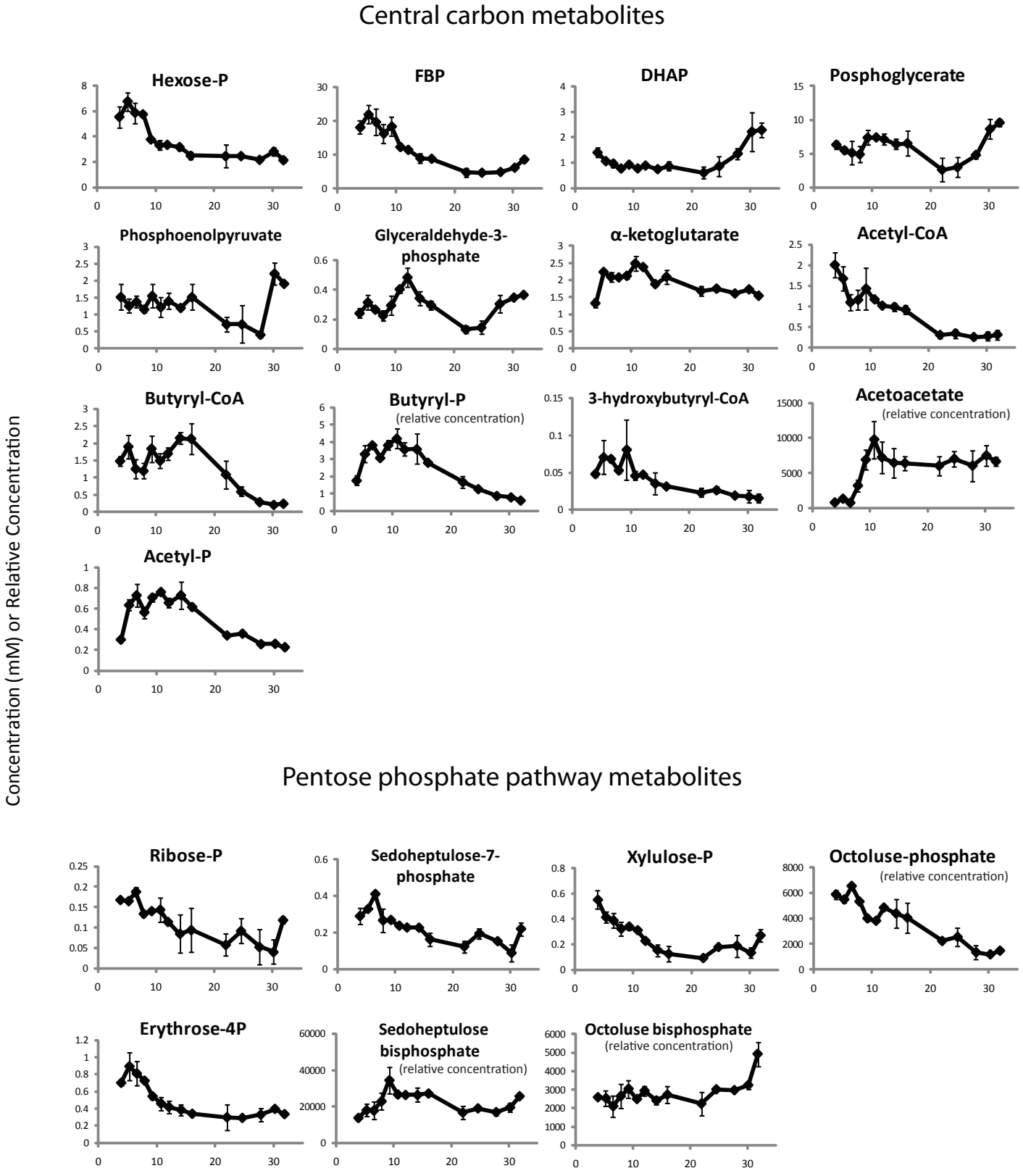

Supplementary Figure 1 (2)

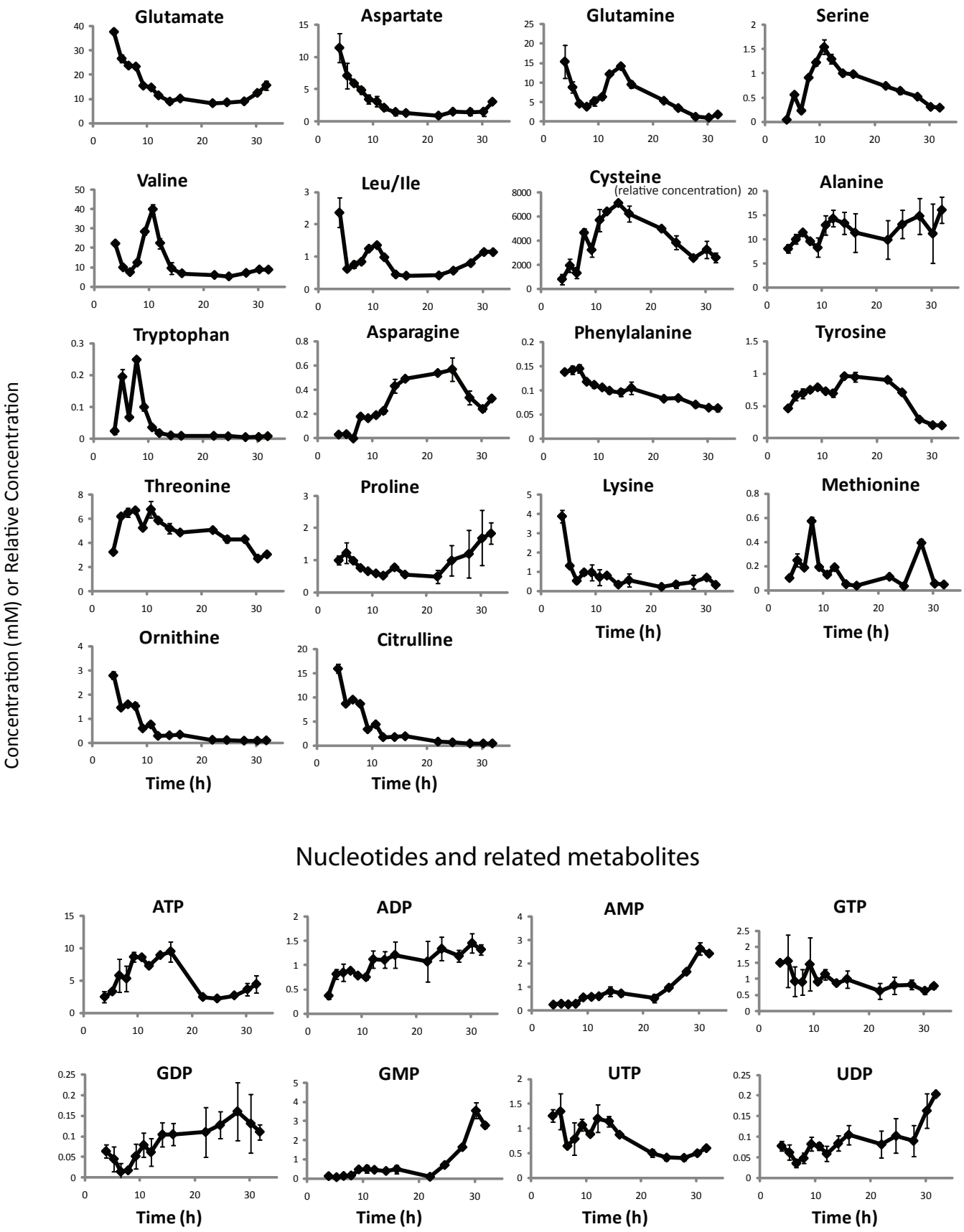

Supplementary Figure 1 (3)

Nucleotides and related metabolites

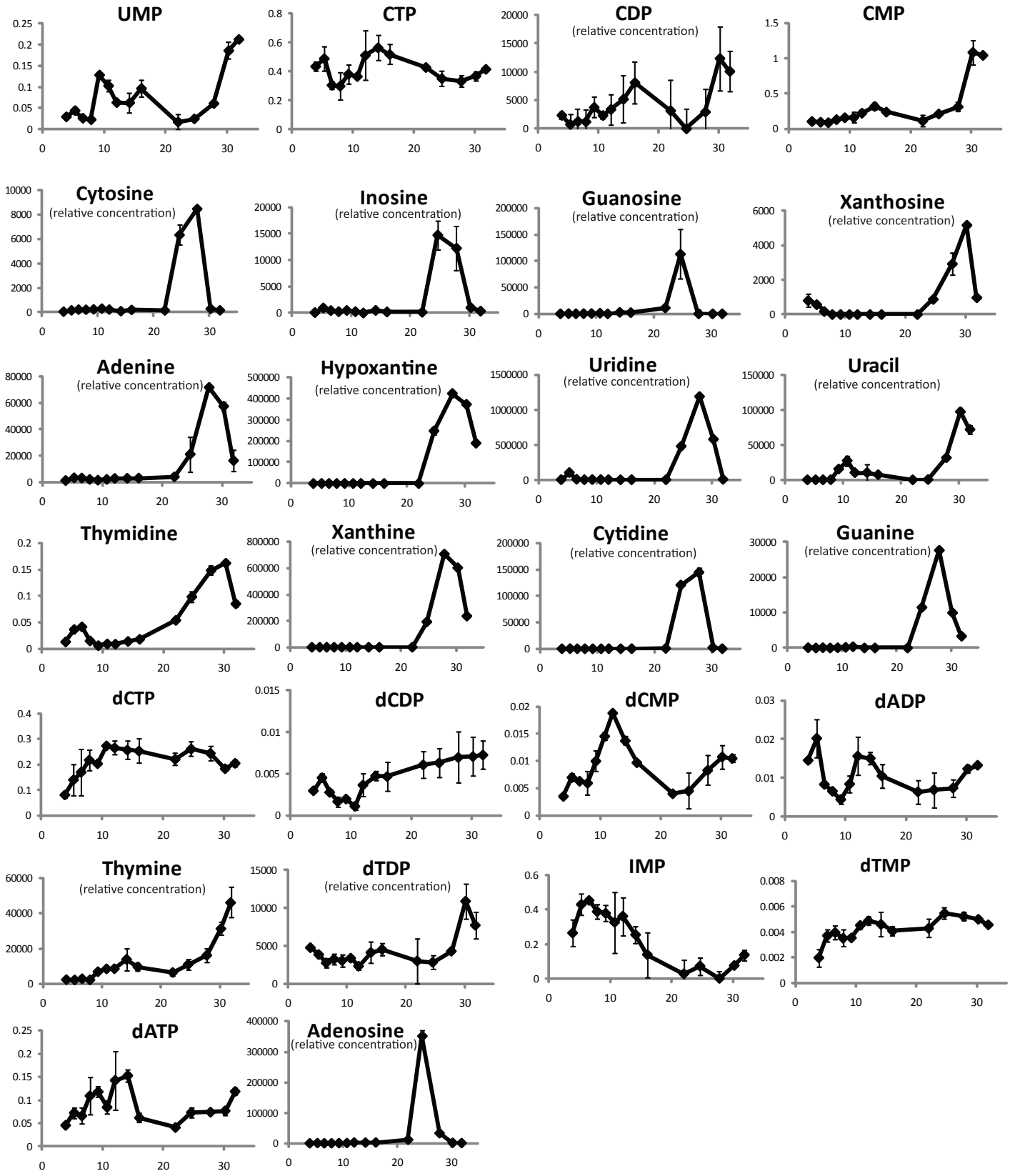

Supplementary Figure 1 (4)

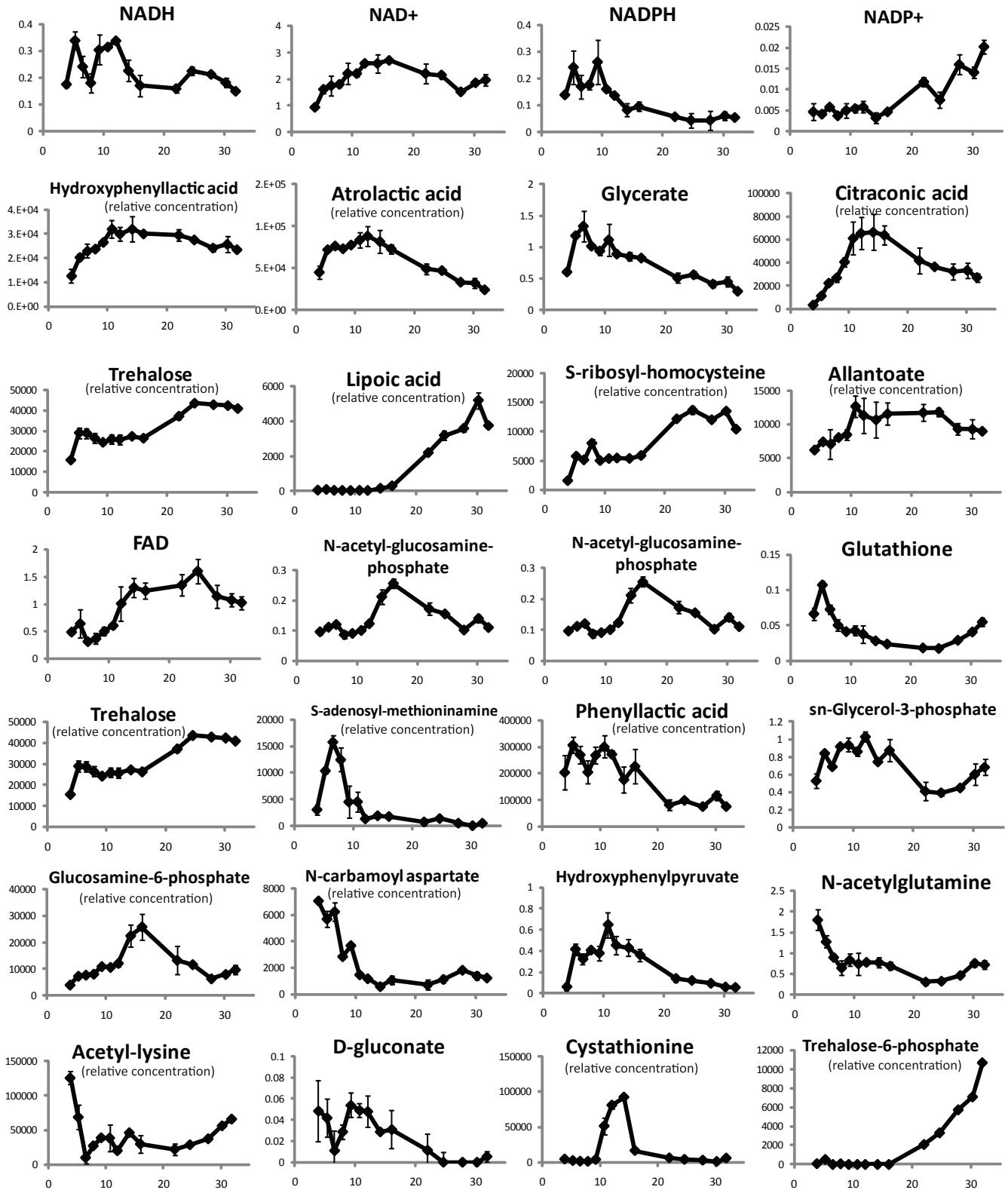

Supplementary Figure 1 (5)

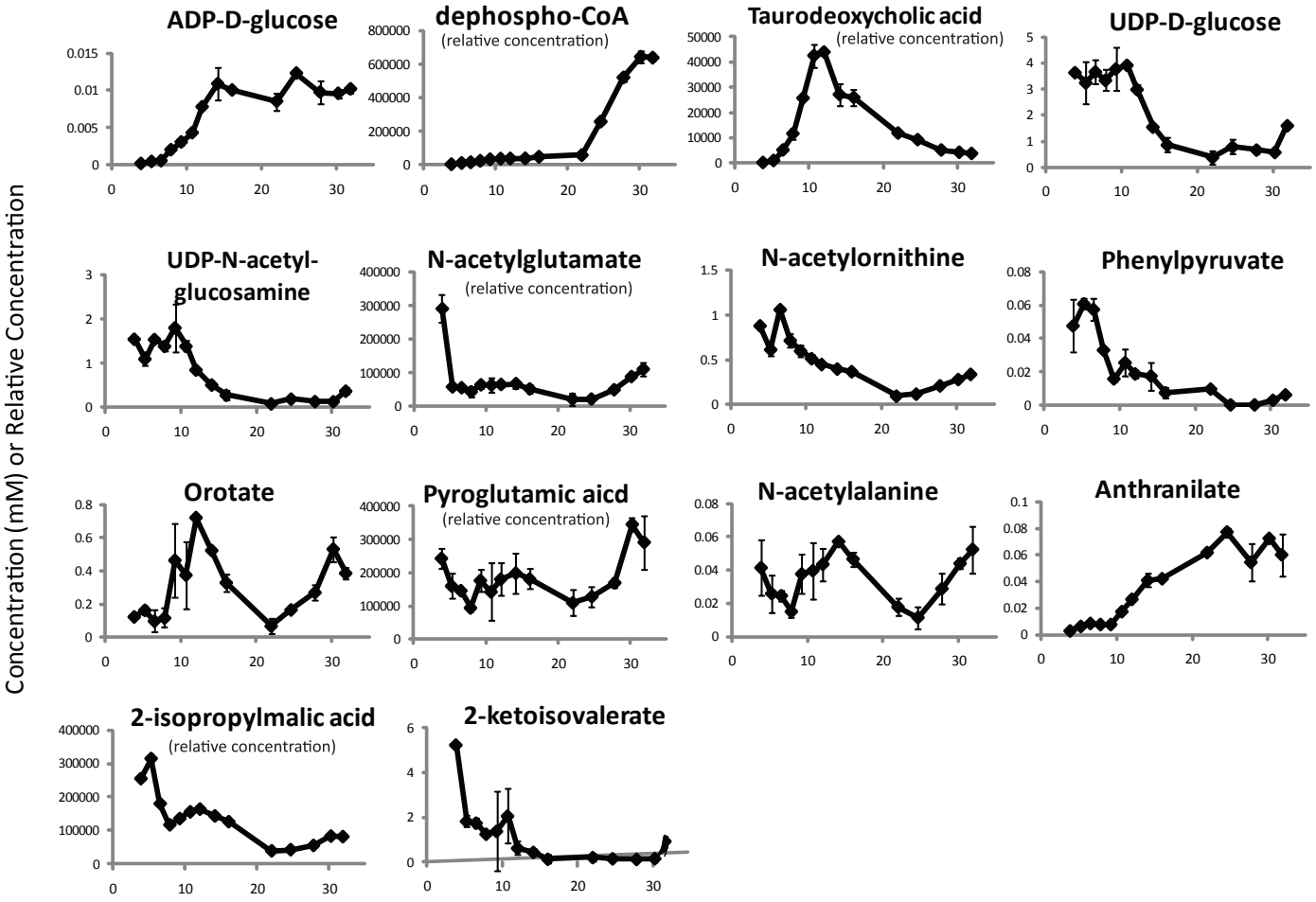

Supplementary Figure 2

A

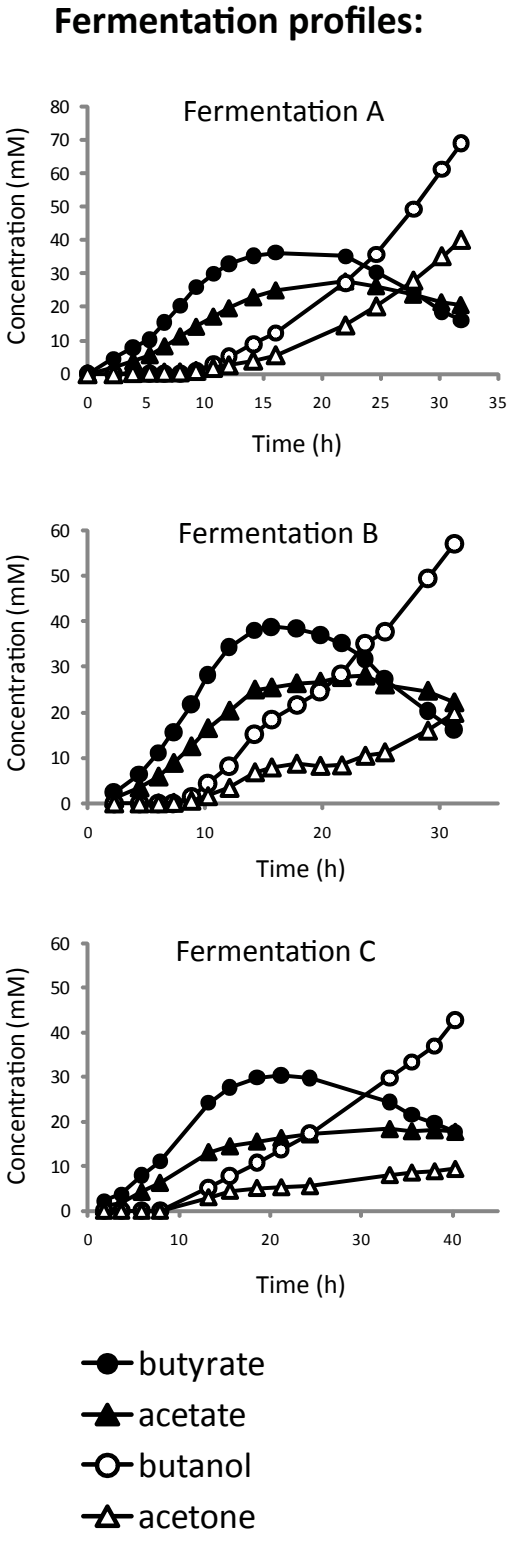

B

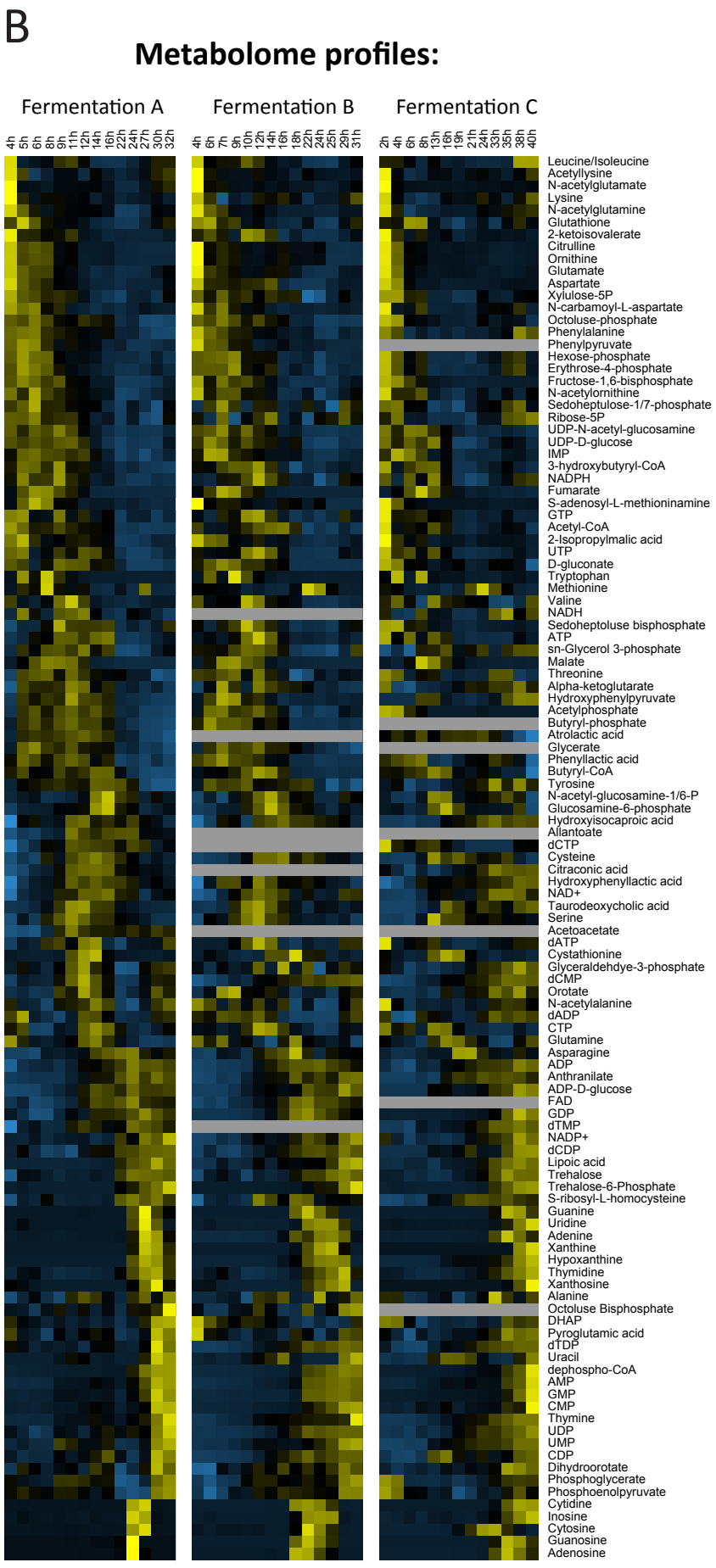

Supplementary Figure 3

Extracellular metabolome profiles:

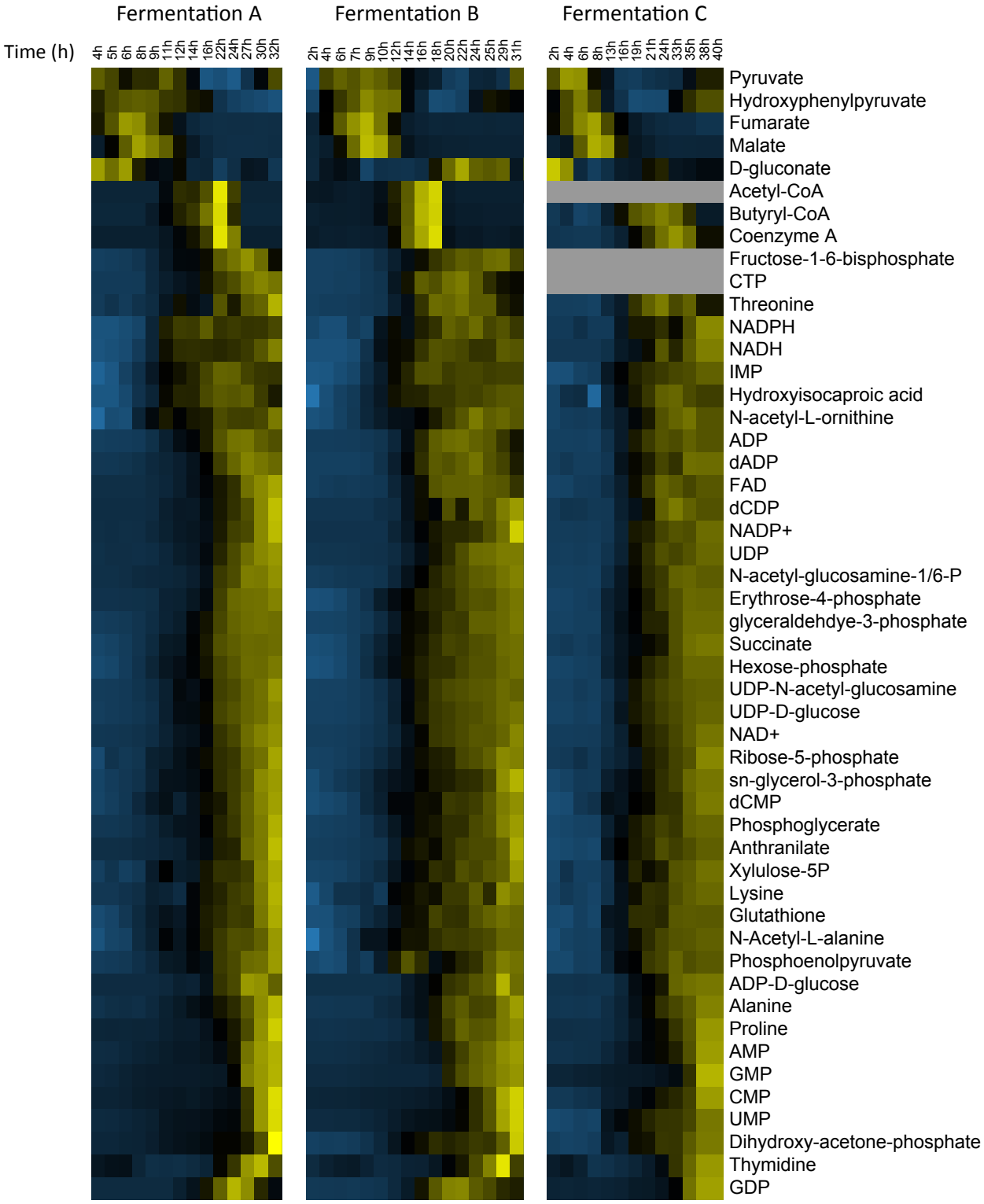

A

Fermentation profiles:

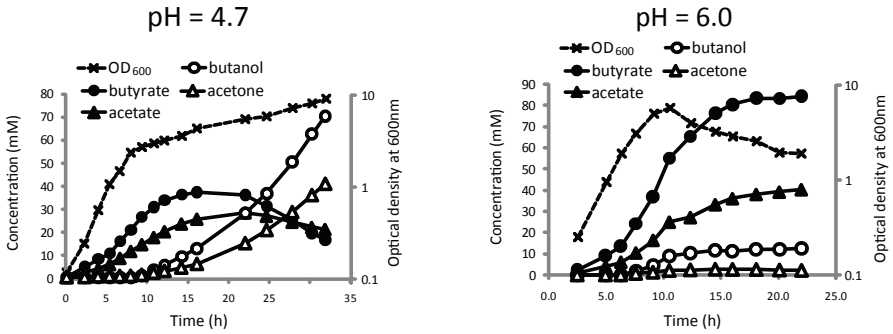

B

Metabolome profiles:

Complete time-course

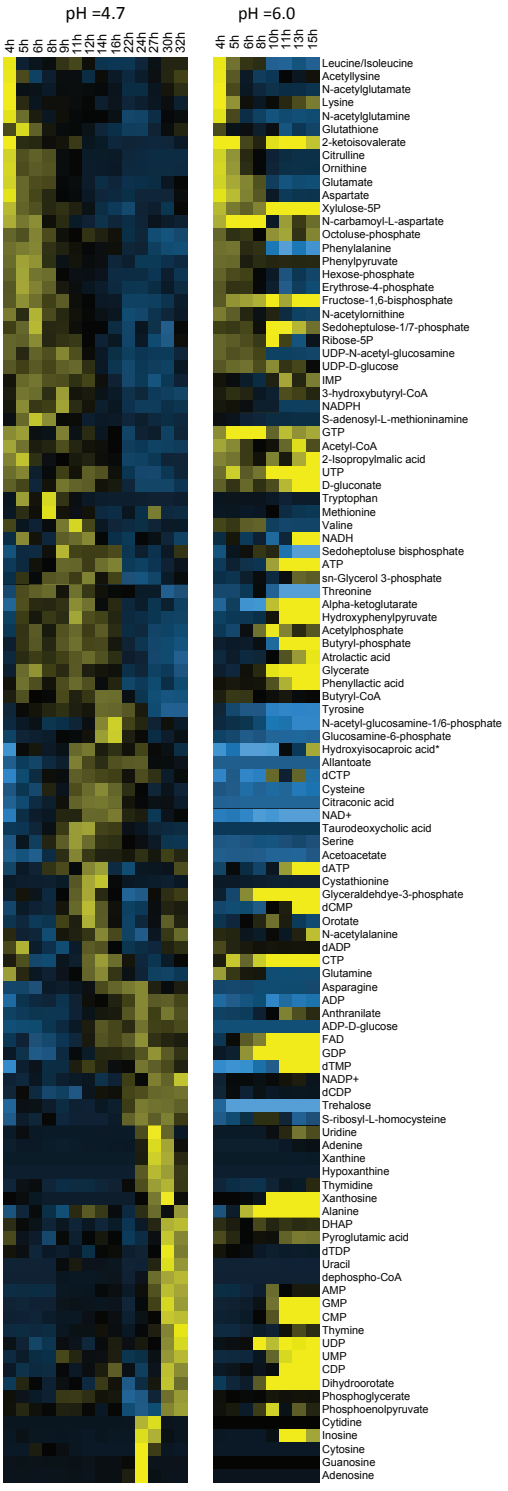

Acidogenic

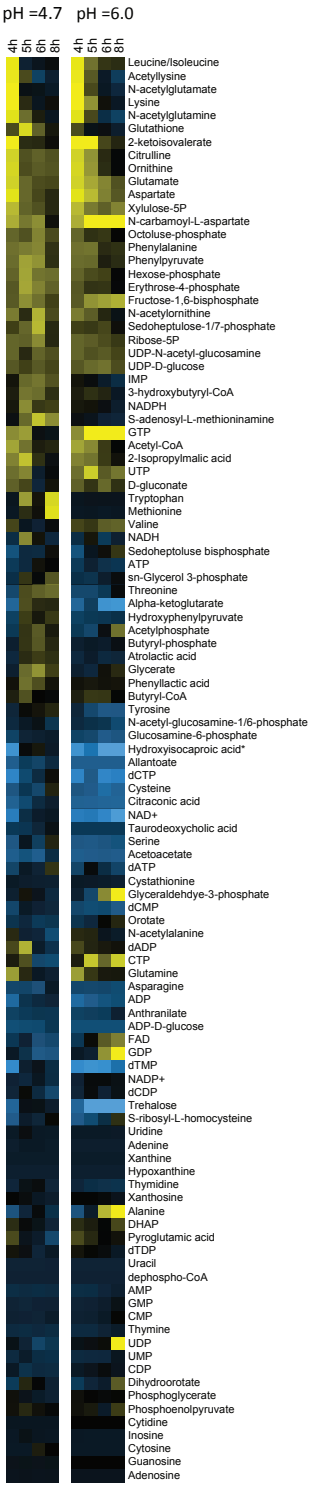

Early solventogenic

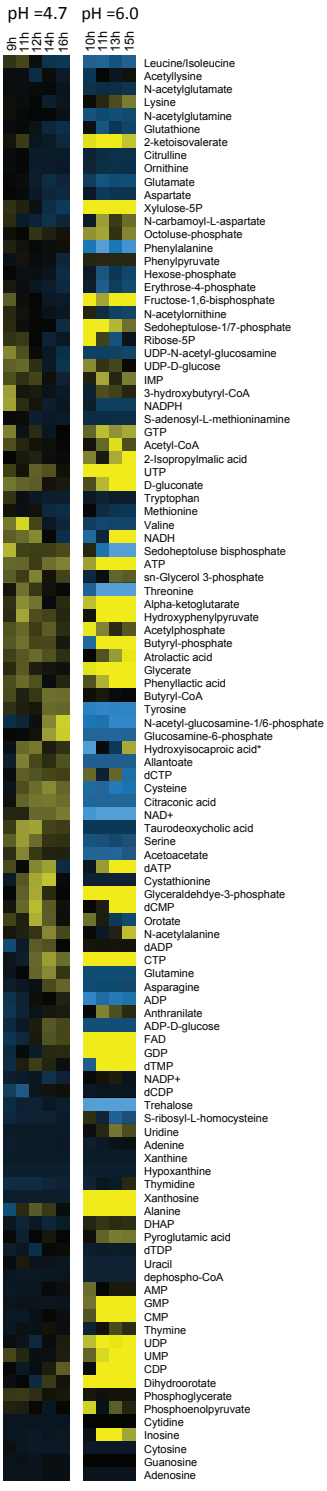

Supplementary Figure 5

A

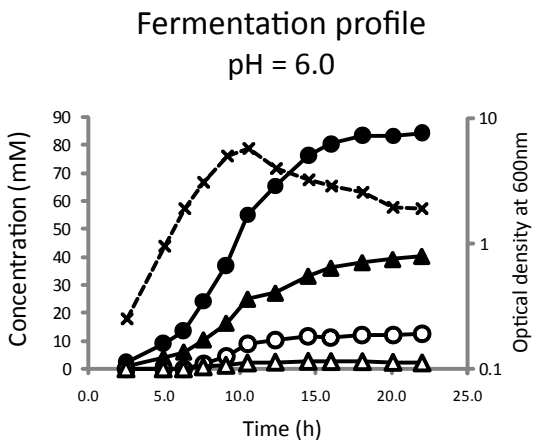

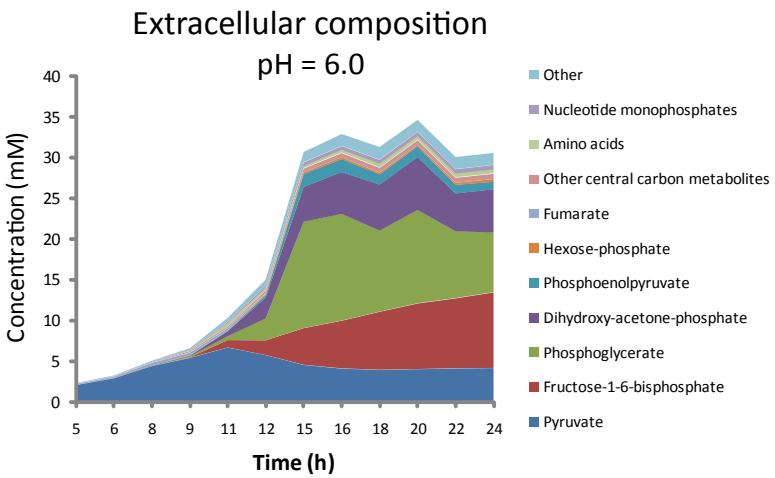

B

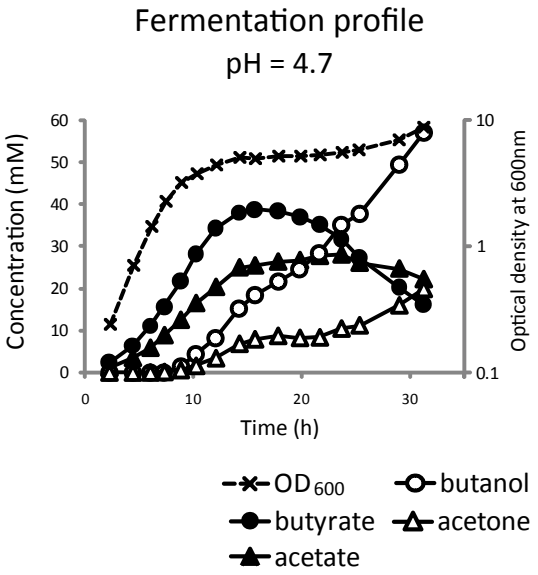

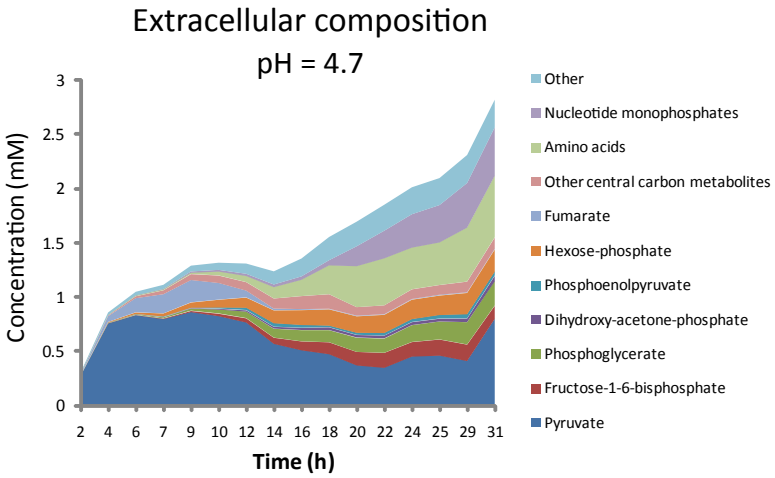

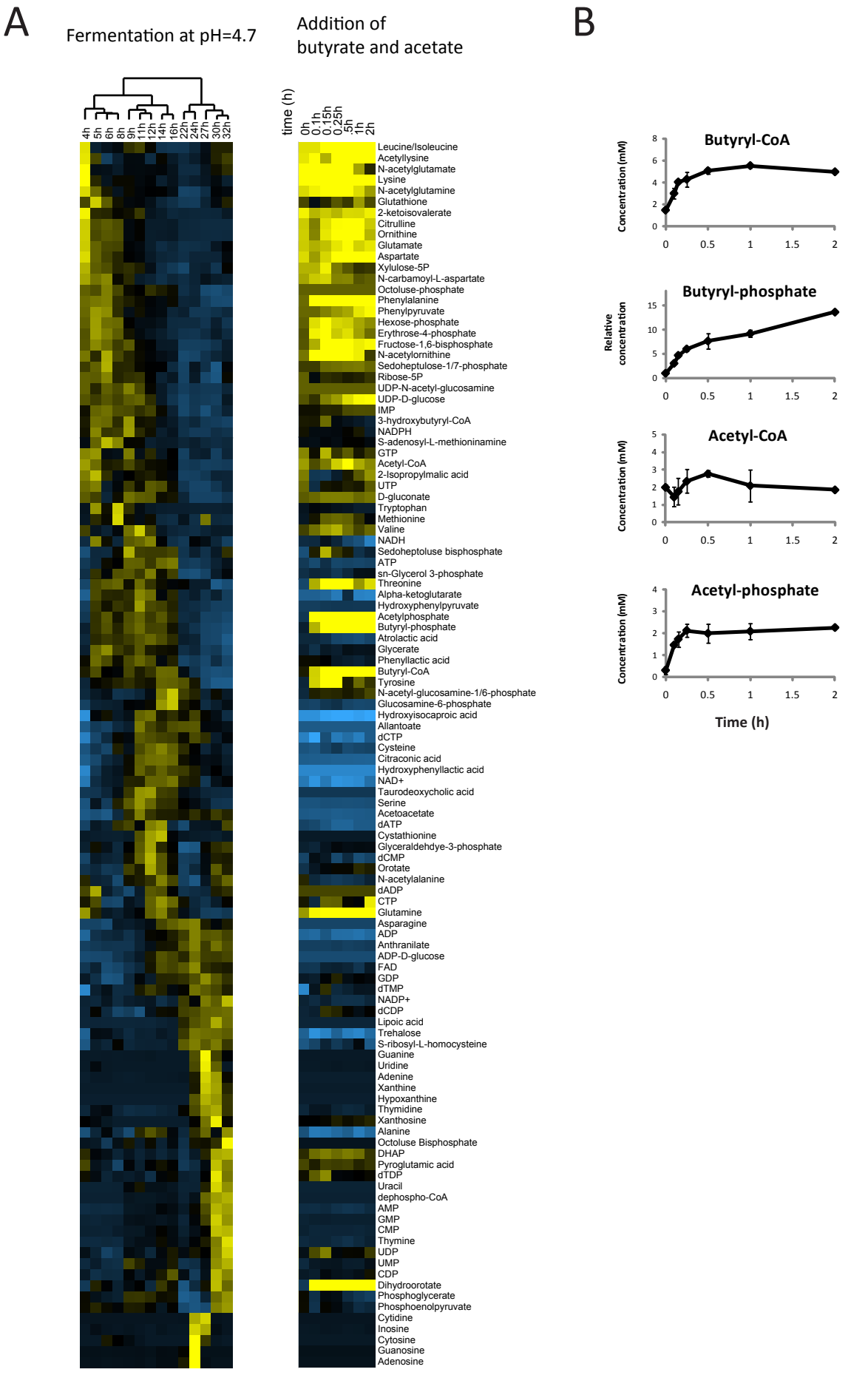
A
Fermentation at pH=4.7
Addition of
butyrate and acetate
4h
5h
6h
8h
9h
11h
12h
14h
16h
22h
24h
27h
30h
32h
time (h)
0h
0.1h
0.15h
0.25h
.5h
1h
2h
Leucine/Isoleucine
Acetyllysine
N-acetylglutamate
Lysine
N-acetylglutamine
Glutathione
2-ketoisovalerate
Citrulline
Ornithine
Glutamate
Aspartate
Xylulose-5P
N-carbamoyl-L-aspartate
Octoluse-phosphate
Phenylalanine
Phenylpyruvate
Hexose-phosphate
Erythrose-4-phosphate
Fructose-1,6-bisphosphate
N-acetylornithine
Sedoheptulose-1/7-phosphate
Ribose-5P
UDP-N-acetyl-glucosamine
UDP-D-glucose
IMP
3-hydroxybutyryl-CoA
NADPH
S-adenosyl-L-methioninamine
GTP
Acetyl-CoA
2-Isopropylmalic acid
UTP
D-gluconate
Tryptophan
Methionine
Valine
NADH
Sedoheptoluse bisphosphate
ATP
sn-Glycerol 3-phosphate
Threonine
Alpha-ketoglutarate
Hydroxyphenylpyruvate
Acetylphosphate
Butyryl-phosphate
Atrolactic acid
Glycerate
Phenyllactic acid
Butyryl-CoA
Tyrosine
N-acetyl-glucosamine-1/6-phosphate
Glucosamine-6-phosphate
Hydroxyisocaproic acid
Allantoate
dCTP
Cysteine
Citraconic acid
Hydroxyphenyllactic acid
NAD+
Taurodeoxycholic acid
Serine
Acetoacetate
dATP
Cystathionine
Glyceraldehdye-3-phosphate
dCMP
Orotate
N-acetylalanine
dADP
CTP
Glutamine
Asparagine
ADP
Anthranilate
ADP-D-glucose
FAD
GDP
dTMP
NADP+
dCDP
Lipoic acid
Trehalose
S-ribosyl-L-homocysteine
Guanine
Uridine
Adenine
Xanthine
Hypoxanthine
Thymidine
Xanthosine
Alanine
Octoluse Bisphosphate
DHAP
Pyroglutamic acid
dTDP
Uracil
dephospho-CoA
AMP
GMP
CMP
Thymine
UDP
UMP
CDP
Dihydroorotate
Phosphoglycerate
Phosphoenolpyruvate
Cytidine
Inosine
Cytosine
Guanosine
Adenosine
B
Butyryl-CoA
Concentration (mM)
Butyryl-phosphate
Relative concentration
Acetyl-CoA
Concentration (mM)
Acetyl-phosphate
Concentration (mM)
Time (h)

Supplementary Figure 7

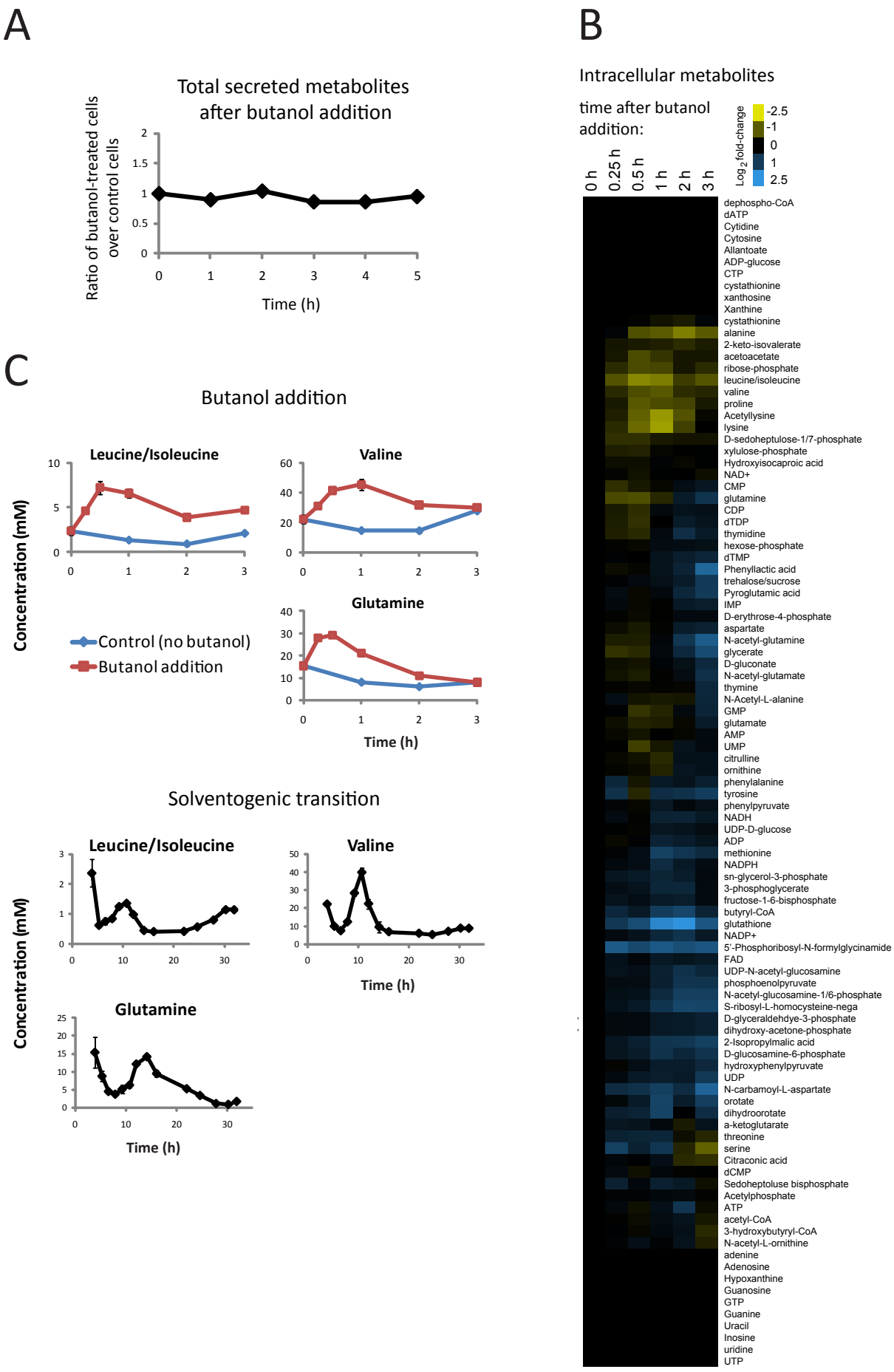

Supplementary Figure 8

A

Assimilation of extracellular ^{13}C-acetate during acidogenesis

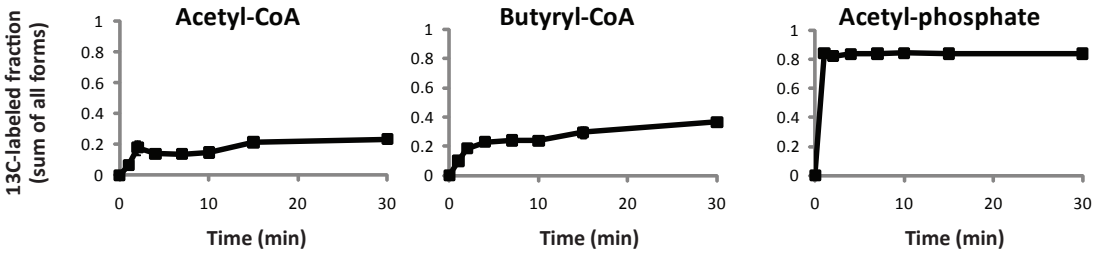

B

Acidogenic cells switched to fresh media containing 100% ^{13}C-glucose

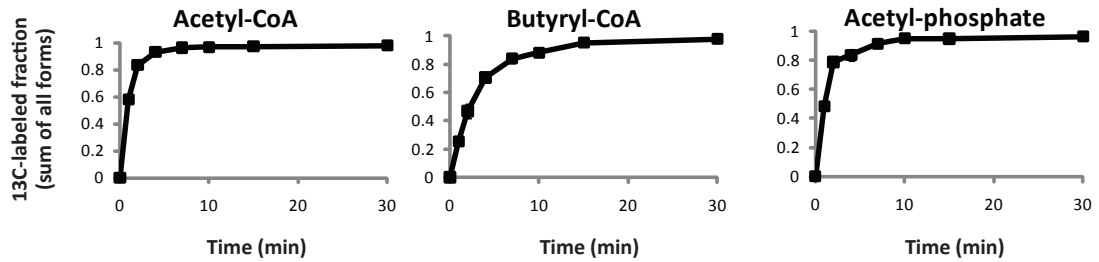

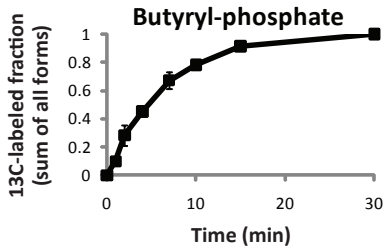

C

Long term assimilation of ^{13}C-glucose during acidogenesis

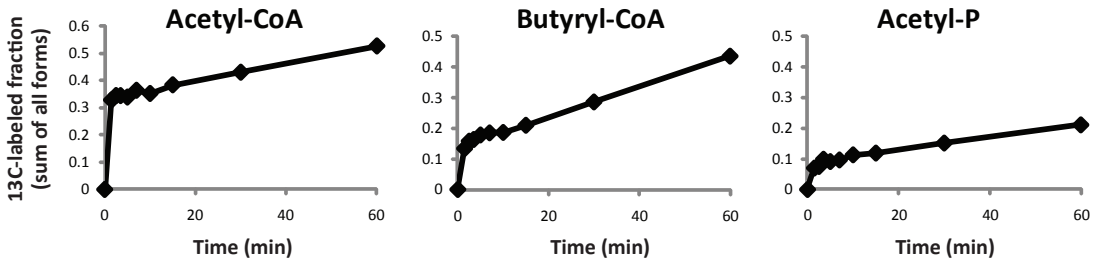

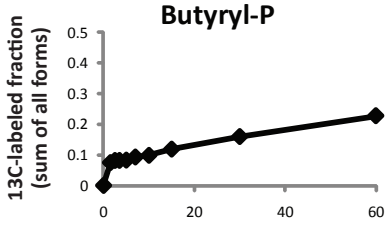

Supplementary Figure 9

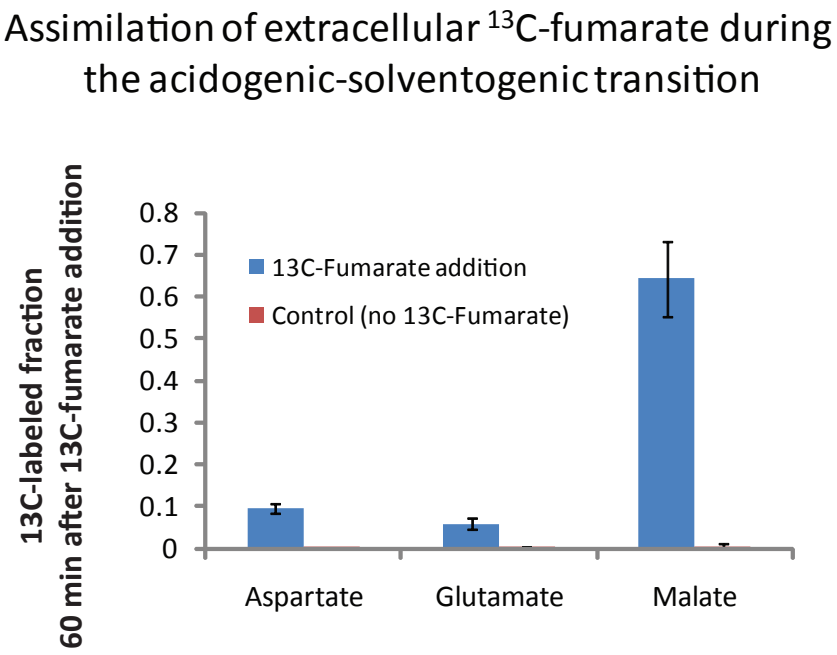

Supplementary Figure 10

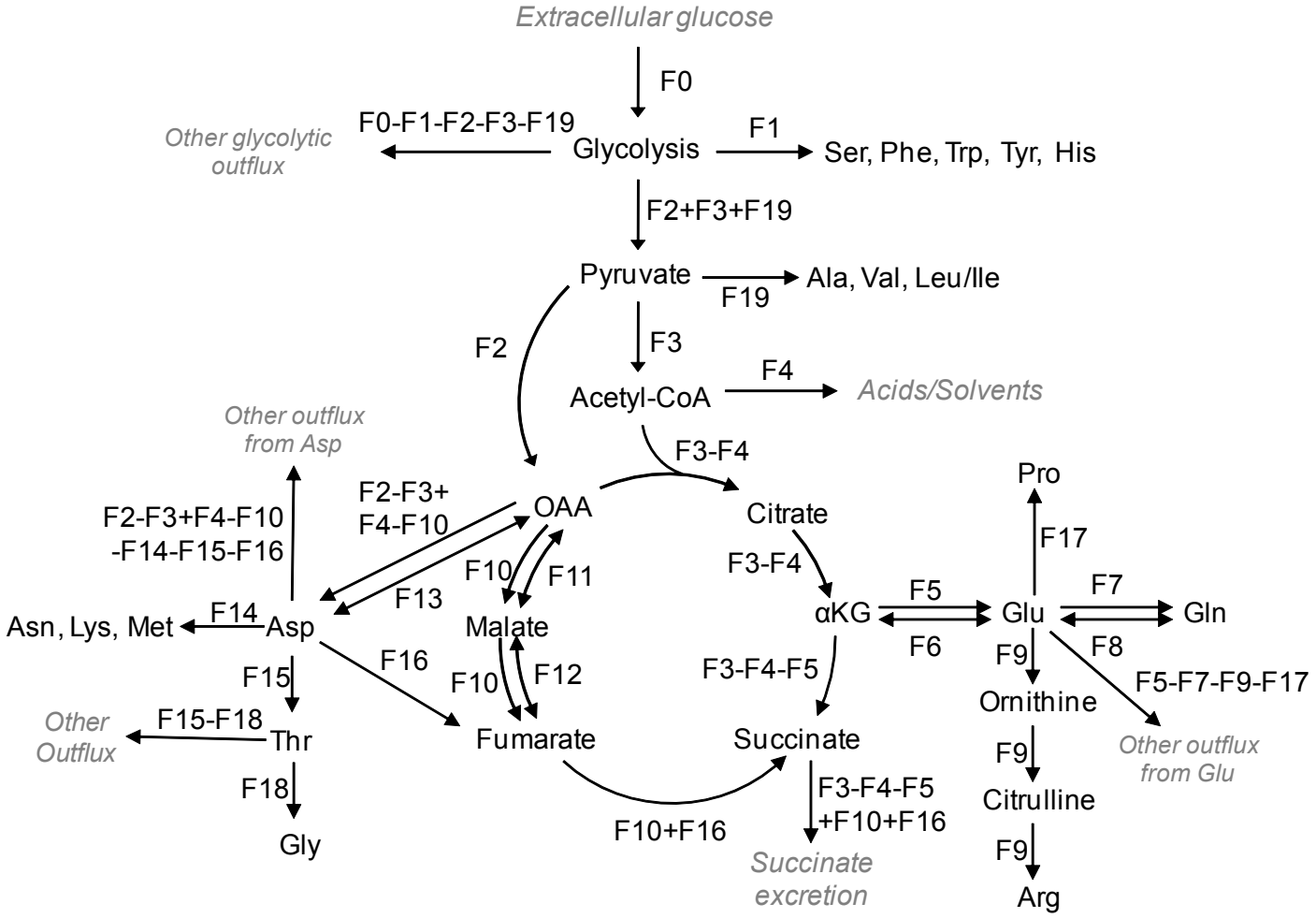

Supplementary Figure 11 (1)

Acidogenic flux distributions, replicate 1

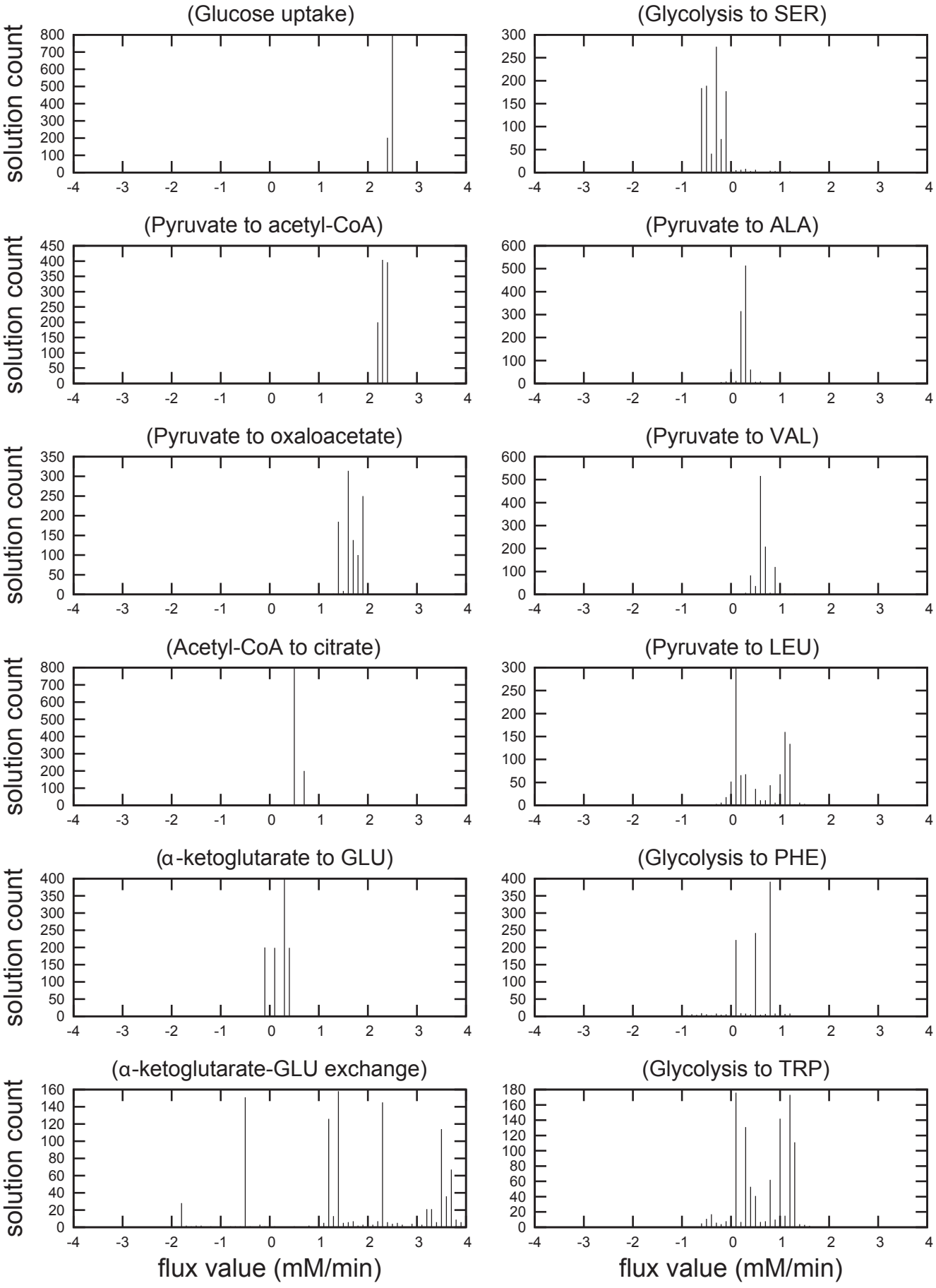

Supplementary Figure 11 (2)

Acidogenic flux distributions, replicate 1

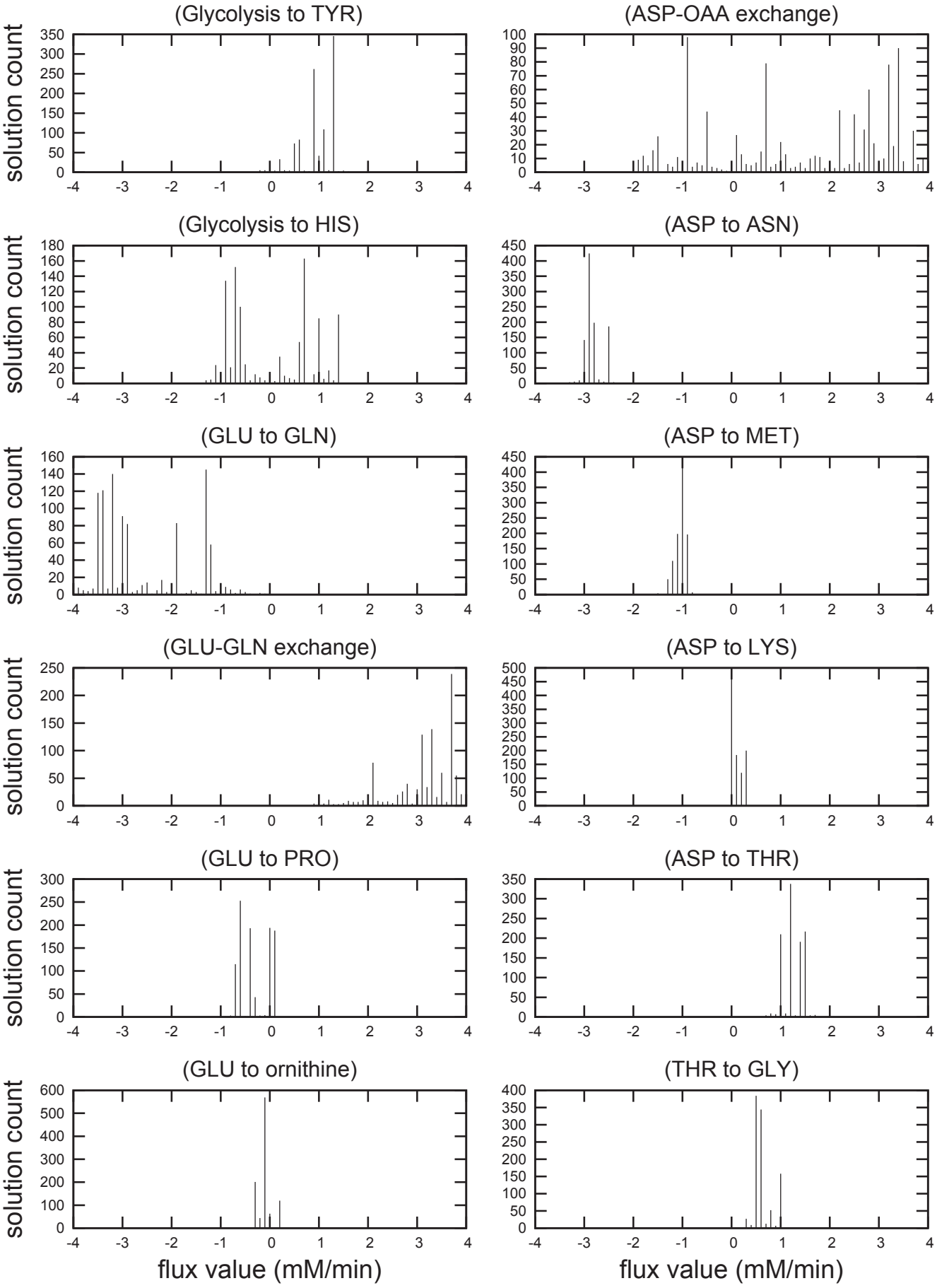

Supplementary Figure 11 (3)

Acidogenic flux distributions, replicate 1

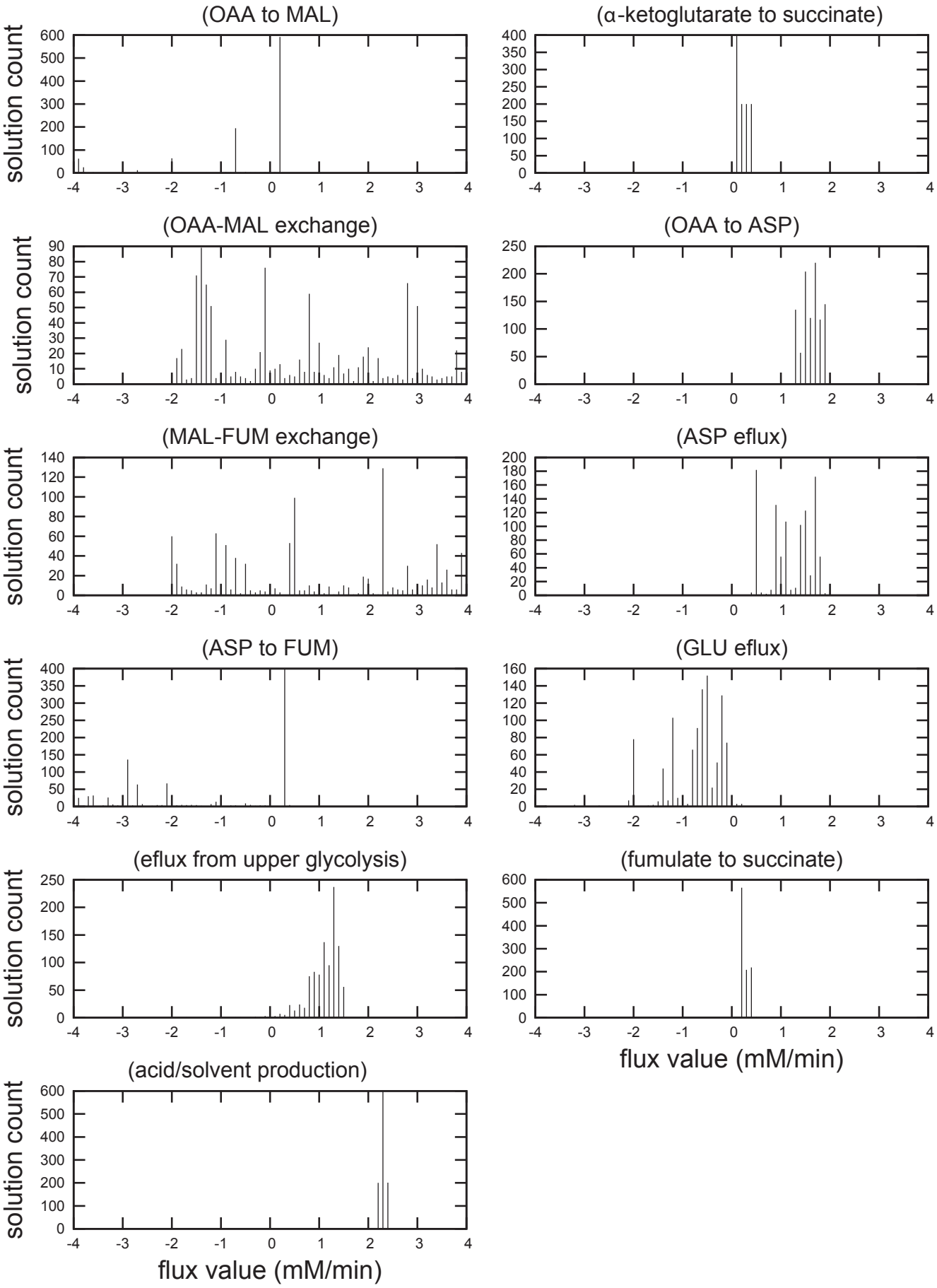

Supplementary Figure 11 (4)

Acidogenic flux distributions, replicate 2

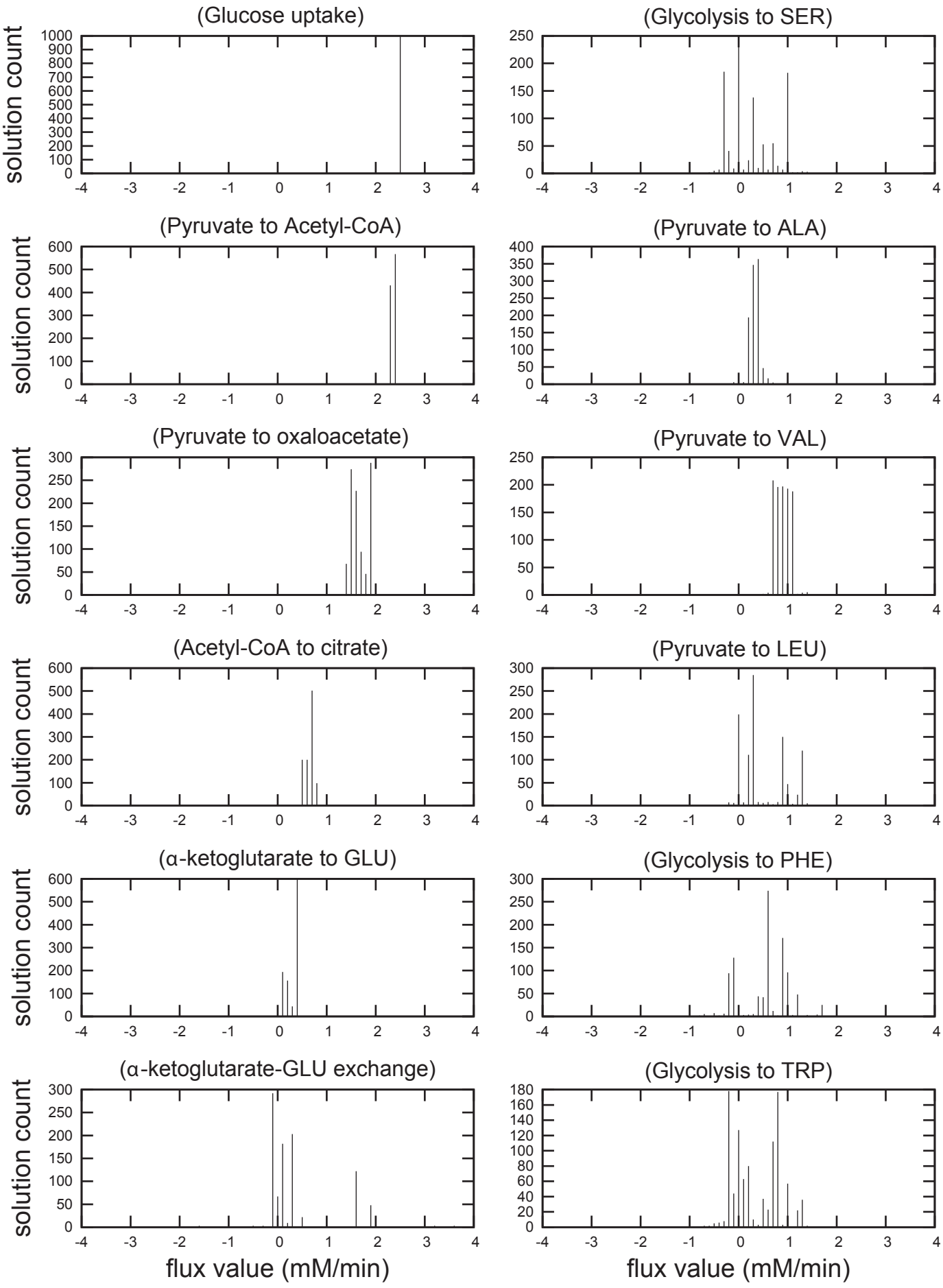

Supplementary Figure 11 (5)

Acidogenic flux distributions, replicate 2

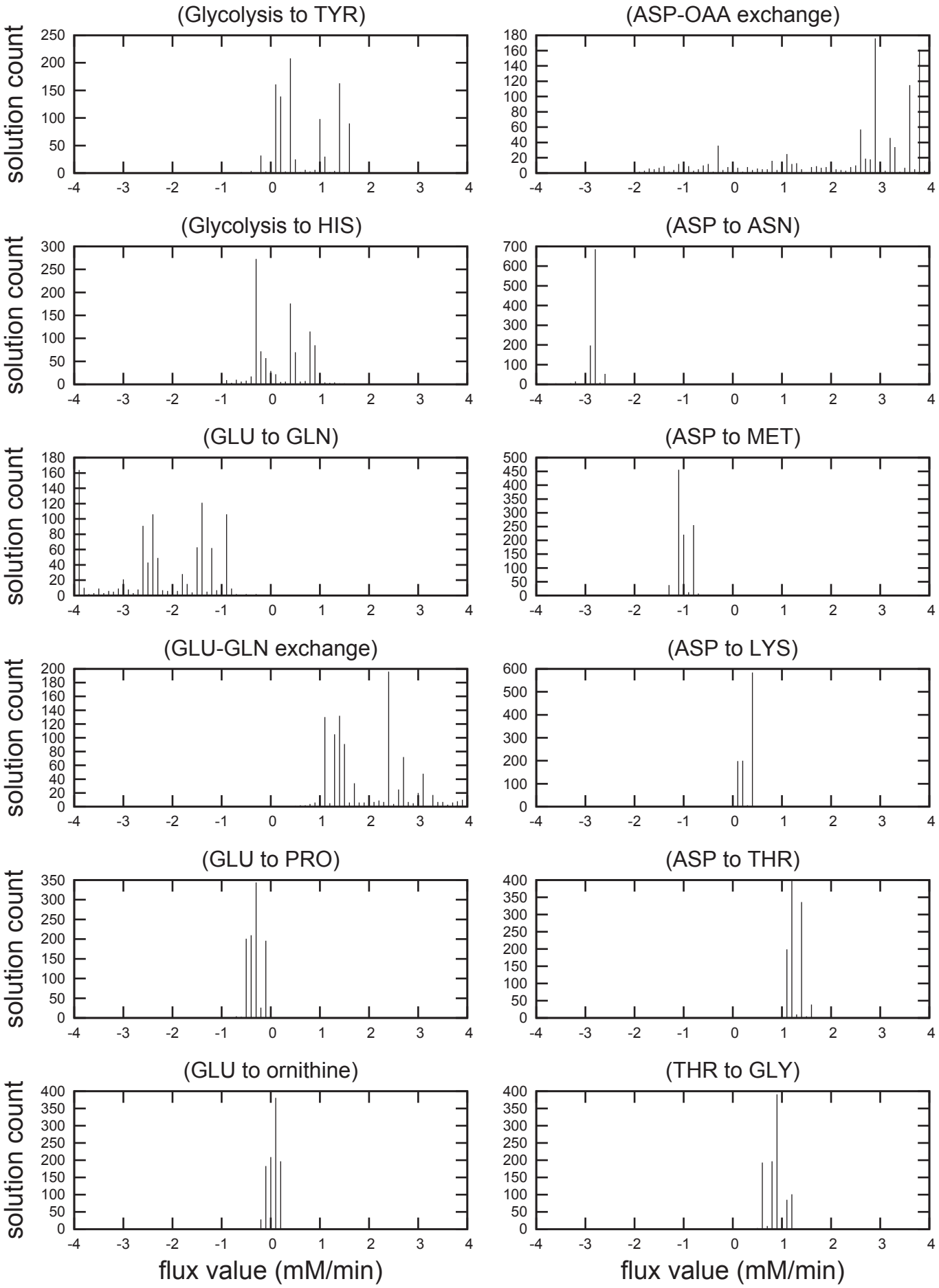

Supplementary Figure 11 (6)

Acidogenic flux distributions, replicate 2

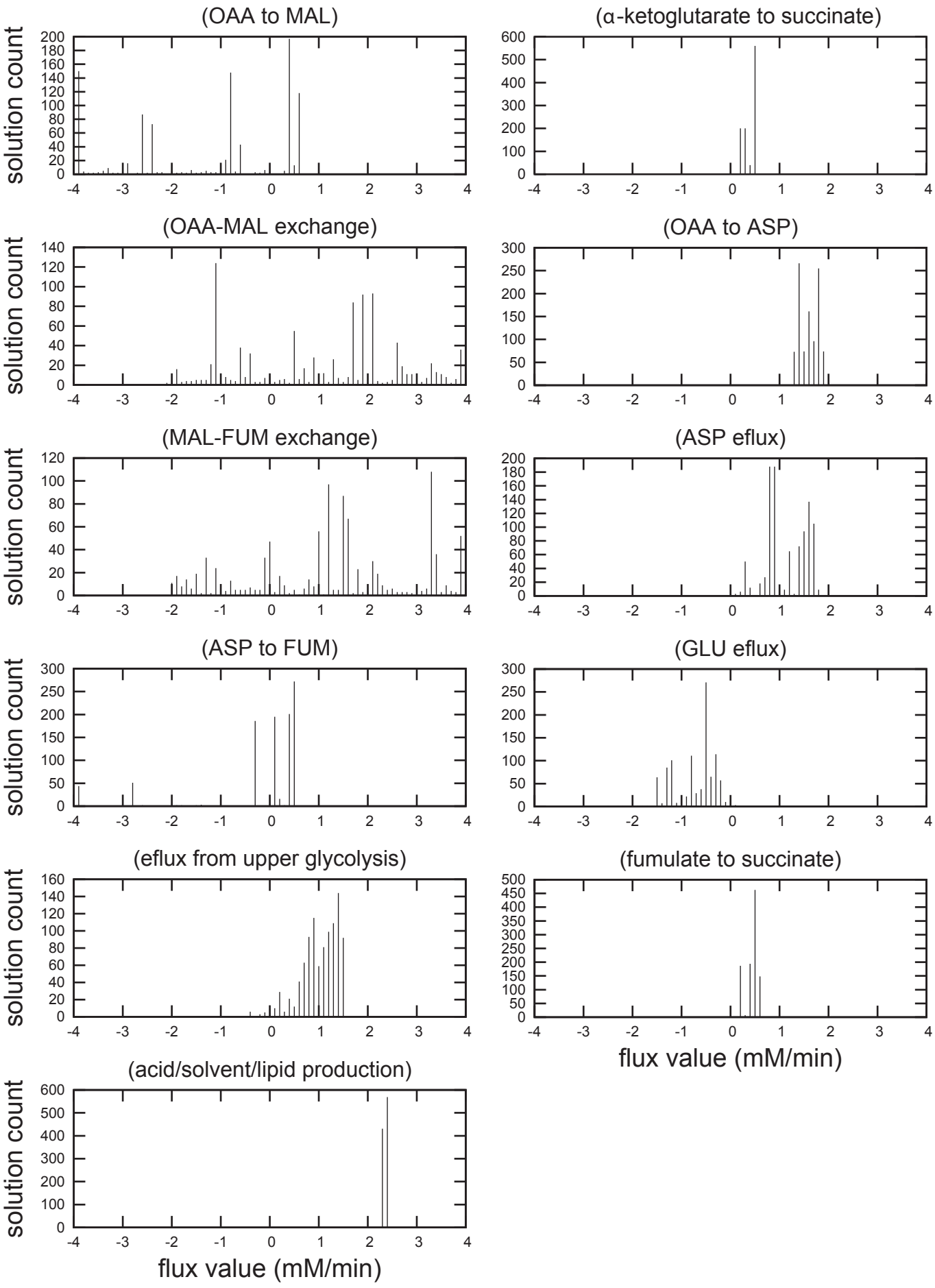

Supplementary Figure 11 (7)

Solventogenic flux distributions, replicate 1

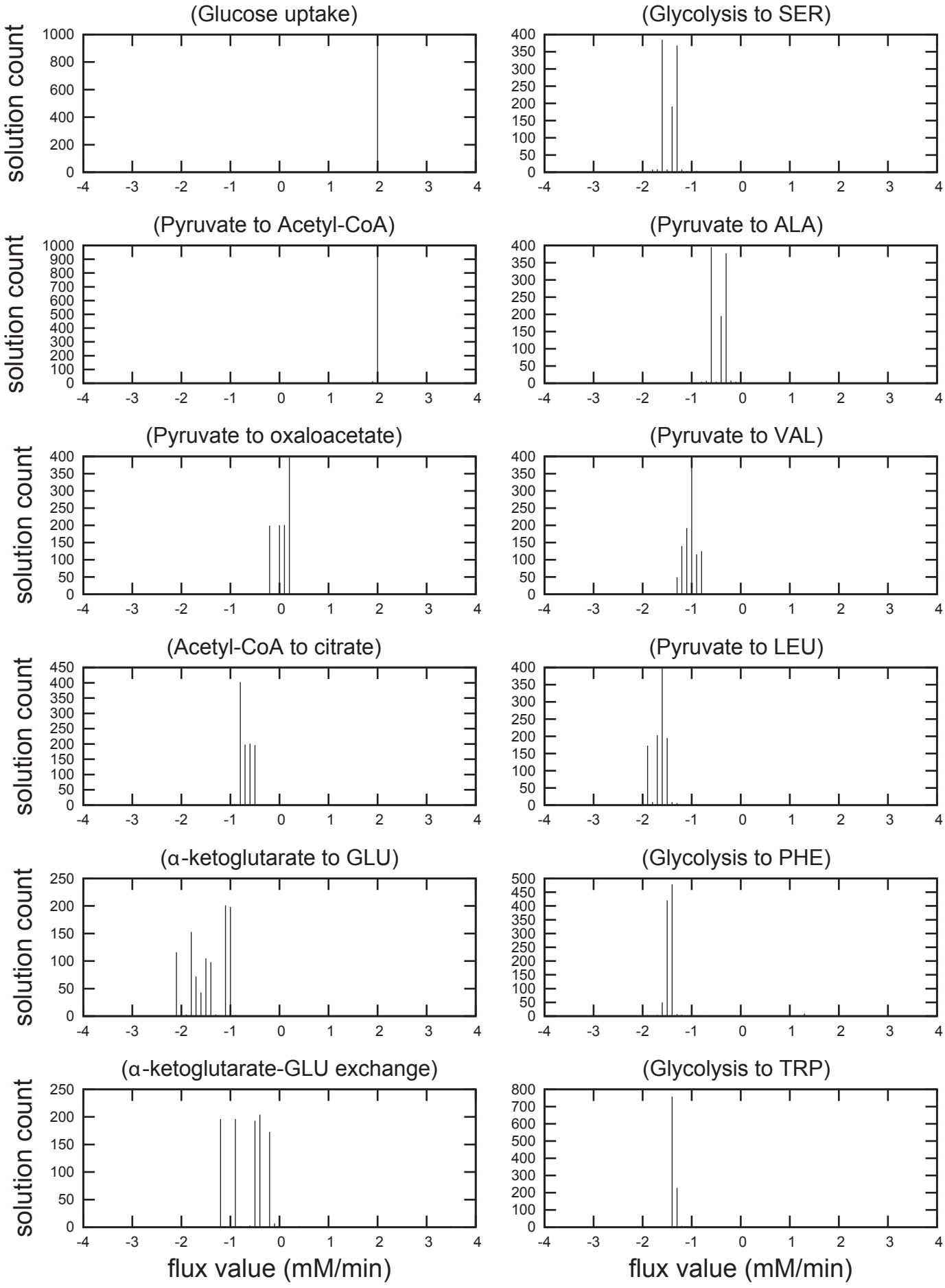

Supplementary Figure 11 (8)

Solventogenic flux distributions, replicate 1

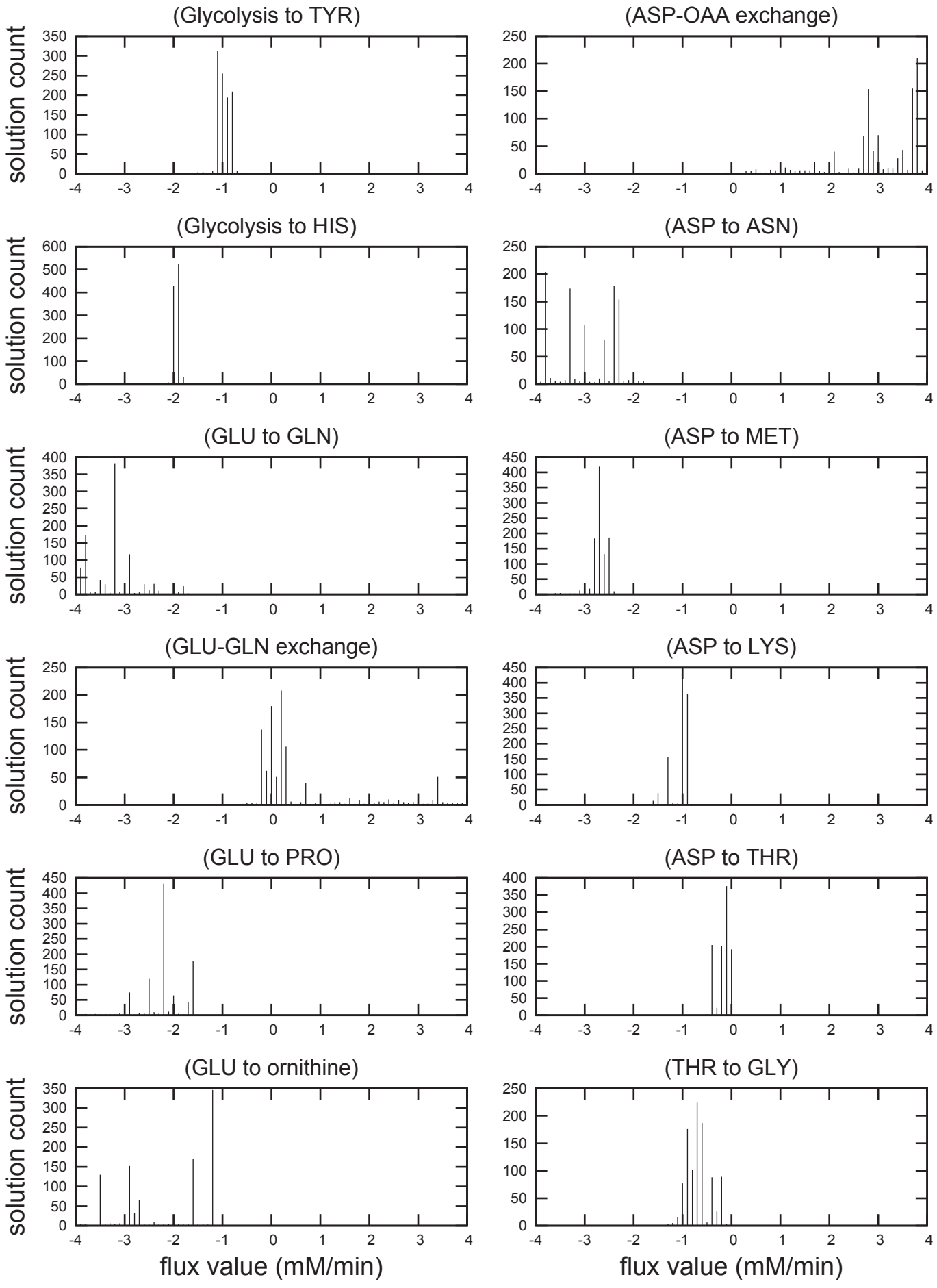

Supplementary Figure 11 (9)

Solventogenic flux distributions, replicate 1

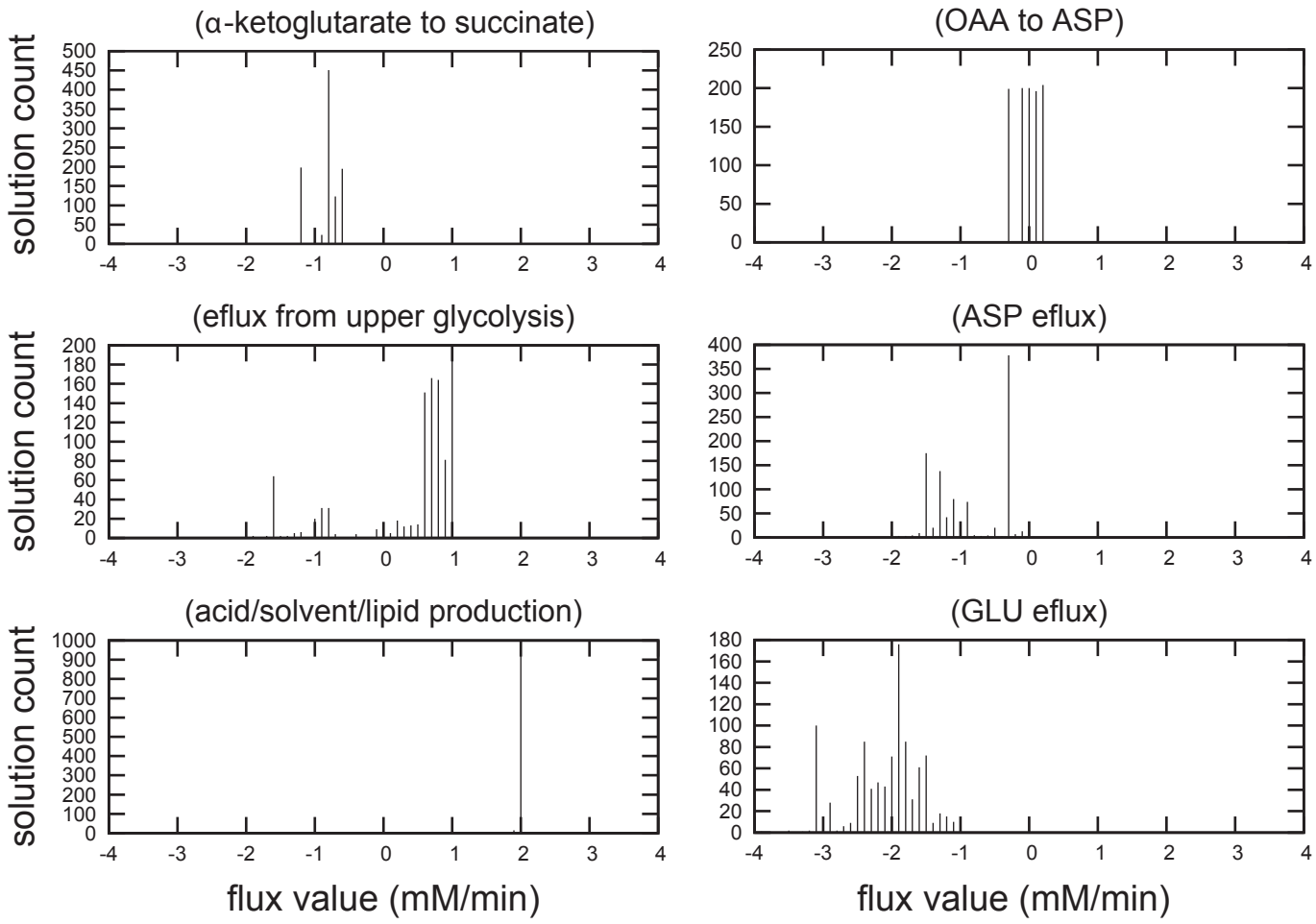

Supplementary Figure 11 (10)

Solventogenic flux distributions, replicate 2

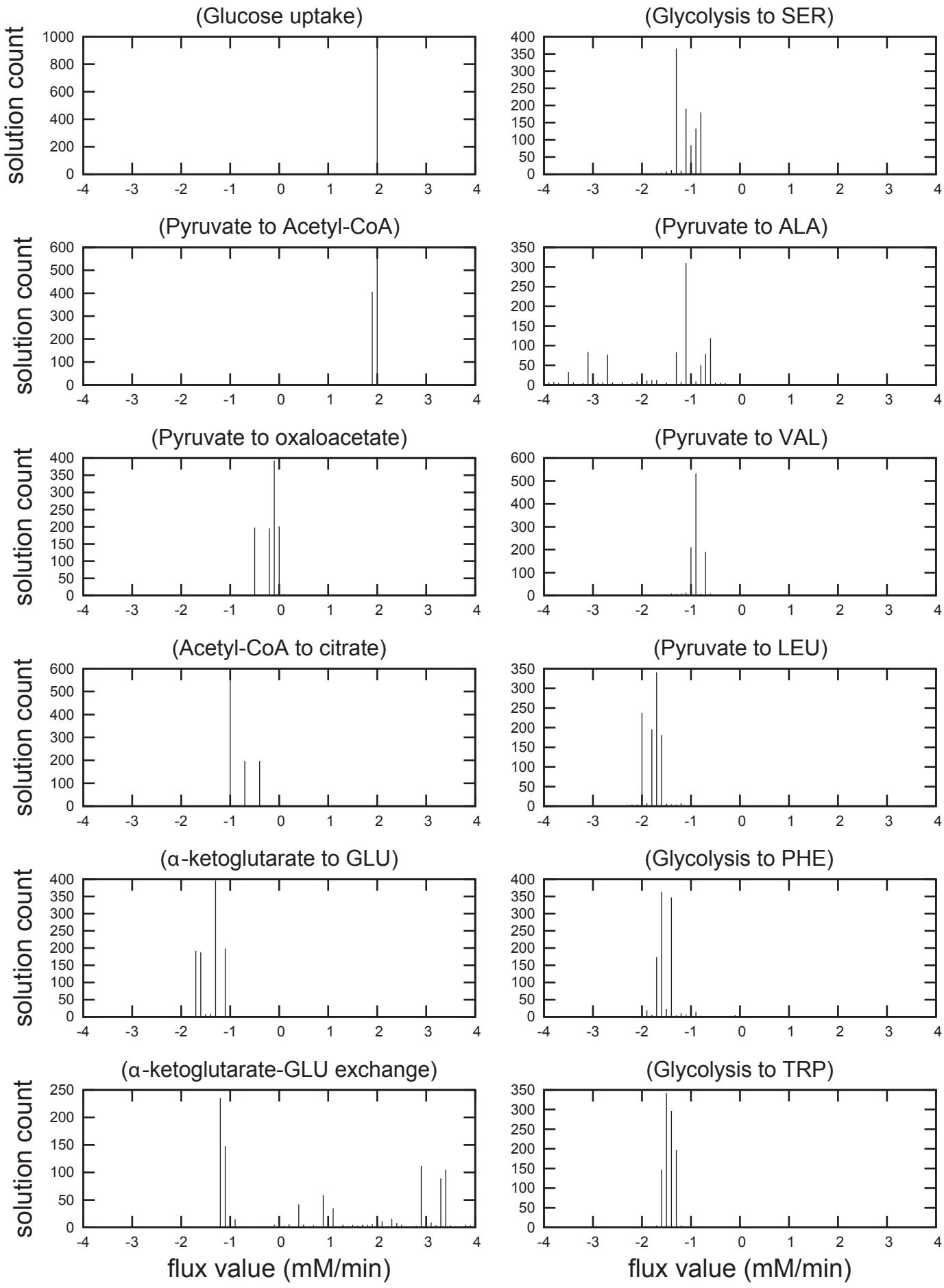

Supplementary Figure 11 (11)

Solventogenic flux distributions, replicate 2

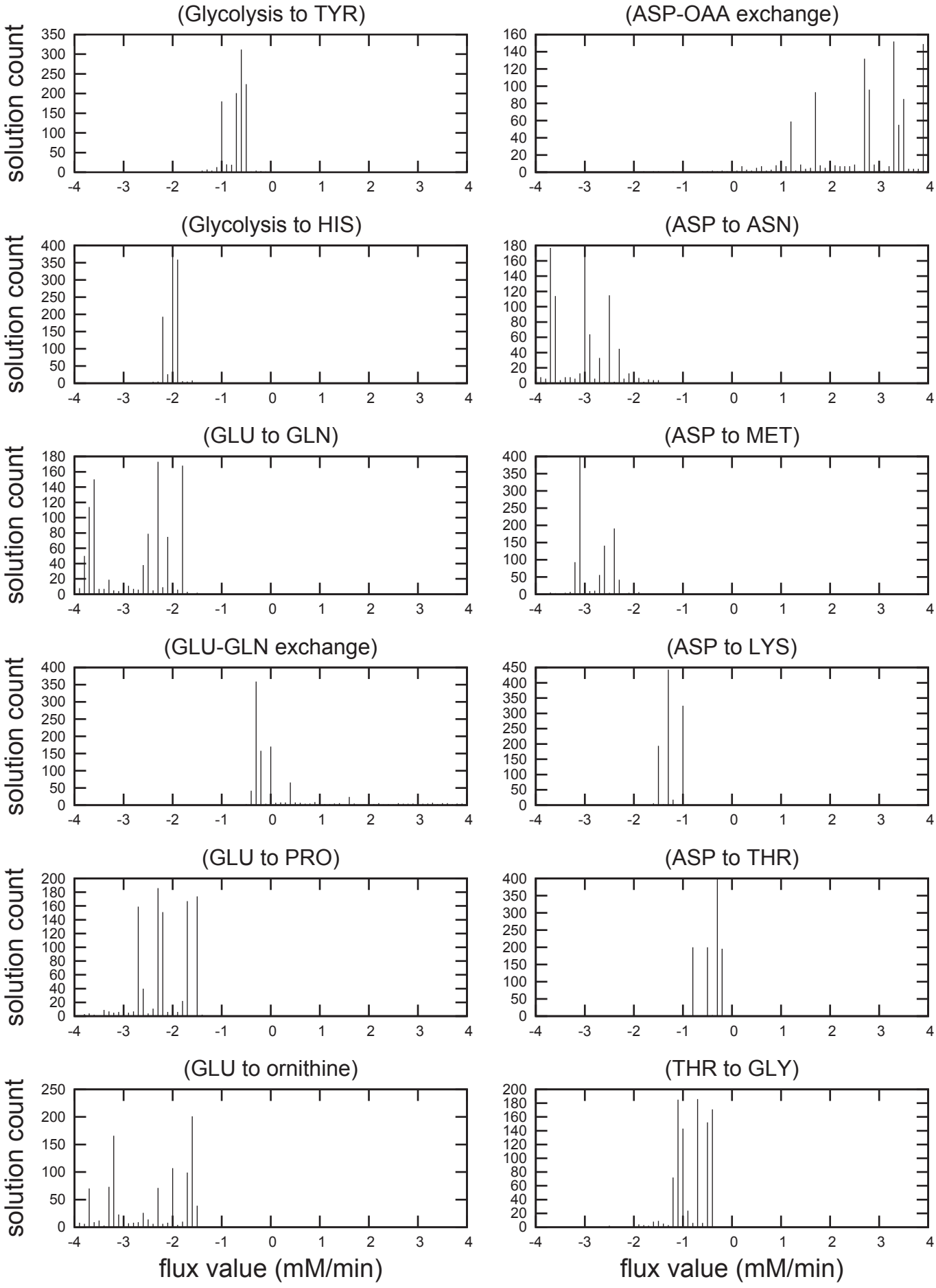

Supplementary Figure 11 (12)

Solventogenic flux distributions, replicate 2